

# Spatial Dynamics of a Diffusive Prey-predator Model with Stage Structure and Fear Effect\*

Nana Zhu<sup>1</sup> and Sanling Yuan<sup>1,†</sup>

**Abstract** To understand the influence of fear effect on population dynamics, especially for the populations with obvious stage structure characteristics, we propose and investigate a diffusive prey-predator model with stage structure in predators. First, we discuss the existence and stability of equilibrium of the model in the absence of diffusion. Then, we obtain the critical conditions for Hopf and Turing bifurcations. Some numerical simulations are also carried out to verify our theoretical results, which indicate that the fear can induce the prey population to show five pattern structures: cold-spot pattern, mixed pattern with cold spots and stripes, stripes pattern, hot-spot pattern, mixed pattern with hot spots and stripes. These findings imply that the fear effect induced by the mature predators plays an important role in the spatial distribution of species.

**Keywords** Prey-predator model, Fear effect, Stage-structured model, Hopf bifurcation, Turing bifurcation, Pattern formation.

**MSC(2010)** 92C10, 92C15.

## 1. Introduction

For a long time, studying the dynamic behaviors of prey-predator models has been a major topic in both ecology and evolutionary biology [23, 26]. It has been long believed that the predators can impact prey populations only through directly killing. However, many theoretical biologists [3, 8, 9] have argued that indirect effects caused by the fear effect induced by predation may play a more important role on the prey population.

Almost all animals respond risk caused by predators and show various anti-predation behaviours such as adjusting foraging behaviors, changing their habitat usage, guard and physiological changes [4, 13, 14, 17]. For example, the prey may choose to give up the primal high-risk habitat and migrate to the low-risk habitat, when they feel risk caused by predators [4], which can cause a large loss if the quality of the low-risk habitats is worse than that of the primal one. In addition, individuals at different stages may be exposed to different levels of risk and therefore react differently. For example, breeding birds will fly away from nests,

---

<sup>†</sup>the corresponding author.

Email address: [Sanling@usst.edu.cn](mailto:Sanling@usst.edu.cn) (S. Yuan), [Nana\\_zhu95@163.com](mailto:Nana_zhu95@163.com) (N. Zhu)

<sup>1</sup>College of Science, University of Shanghai for Science and Technology, Shanghai 200093, China

\*The authors were supported by National Natural Science Foundation of China (No. 12071293).

leaving immature birds in danger and taking less care of them, as the mature birds feel dangerous. Even the transient absence of mature birds may lower survival probability of immatures, because immatures may undergo less suitable living environment and face more higher risk of predators [4]. In that case, although the odds of survival for mature birds have increased in short-term, the whole fitness of birds species will decrease, because the fear by predation may cause a reduction in their reproduction [20]. Zanette [24] also conducted some field experiments on song sparrows throughout the breeding season, using electric fences to test direct predation on both young and adult song sparrows. There is no directly killing in all experiments, but the vocal cues of the predators broadcast were used to imitate predation risk in the wild. They tested two groups of female song sparrows, among which one group was exposed to the predator sounds, and the other one was not. The researchers [24] found the one exposed to the predators voice reduced 40 percent fewer offspring than the other group, because fewer eggs were laid and fewer nestlings survived. Therefore, the anti-predator behaviour of prey may be helpful in increasing the probability of survival in a short term, but can cause large costs on reproduction in the long term [4].

On the other hand, the predators may also exhibit different predation abilities at different stage of their growth. For example, there exists a type lion living in South America. Only the mature lions can attack and capture buffaloes as their food, while the immature lions get living resources depending on their parents because they have no ability to attack the buffaloes until they become almost one year old [15]. Notice that in this situation, the fear perceived by prey is only from the mature predators. Therefore, it is essential to divide the predator individuals into different stages when modeling the interaction dynamics between prey and predators. As far as we know, the models with stage structure in prey-predator population have been widely investigated in the following pieces of literature (see e.g., [1, 5, 10, 25]). However, there are relatively few investigations for the stage structure predator-prey models with fear effect, especially for the diffusive predator-prey models with both fear effect and stage structure in predators. To this end, in this paper, we will focus on exploring the influence of fear induced by mature predators on the spatial distribution of prey species by discussing a diffusive prey-predator model with stage structure in predators.

Let  $u(x, t)$ ,  $v_1(x, t)$ , and  $v_2(x, t)$  be respectively the densities of the prey, the juvenile and mature predators at position  $x$  and time  $t$ . We suppose the prey population grows logistically in the absence of predators, i.e., the per capita rate of prey is  $r(1 - \frac{u}{m})$ , where  $r$  is the intrinsic growth rate of the prey,  $m$  is the environmental carrying capacity for the prey population. The mature predators catch the prey by complying with Holling-type II functional response  $\frac{auv_2}{b+u}$  [6], where  $a$  stands for the maximal prey consumption rate of a mature predator individual,  $b$  represents the half-saturation constant. Since only the mature predators can attack the prey species, the fear perceived by prey is just from the mature predators. Thus, the fear function can be written as  $\frac{1}{1+k_1v_2}$ , where  $k_1$  stands for the fear level, and therefore, the prey population grows with the rate of  $\frac{ru}{1+k_1v_2}(1 - \frac{u}{m})$ . Assume that  $c$  is the per capita birth rate of predators, then  $\frac{cav_1v_2}{b+u}$  describes the birth rate of the juvenile predators. As we know, not all the juvenile predators can mature into adults, say the lions in South America we have mentioned above. We suppose the maturation rate of the juvenile predators as  $\alpha$  and their death rate is  $q_1$ . Moreover, following [2], we assume that the death rate of mature predators is

mainly dominated by their crowding effect, i.e., the mature predators die at rate  $q_2 v_2^2$ . It is well-known that, in the real ecosystem, both the prey and the predators move randomly and their densities and distributions depend on the location [21]. Therefore, it is necessary to consider the diffusion of the individuals into our model, and suppose the self-diffusion coefficients of the prey, juvenile and mature predators are respectively  $d_{11}$ ,  $d_{22}$  and  $d_{33}$ . Biologically, we assume that all the parameters above are positive. Our model can be formulated as follows:

$$\begin{cases} \frac{\partial u}{\partial t} = d_{11} \Delta u + \frac{ru}{1+k_1 v_2} \left(1 - \frac{u}{m}\right) - \frac{a u v_2}{b+u}, & x \in \Omega, t > 0, \\ \frac{\partial v_1}{\partial t} = d_{22} \Delta v_1 + \frac{c a u v_2}{b+u} - (\alpha + q_1) v_1, & x \in \Omega, t > 0, \\ \frac{\partial v_2}{\partial t} = d_{33} \Delta v_2 + \alpha v_1 - q_2 v_2^2, & x \in \Omega, t > 0, \\ \frac{\partial u}{\partial \vec{v}} = 0, \frac{\partial v_1}{\partial \vec{v}} = 0, \frac{\partial v_2}{\partial \vec{v}} = 0, & x \in \partial \Omega, t > 0, \\ u(x, 0) = u_0(x) \geq 0, v_1(x, 0) = v_{10}(x) \geq 0, v_2(x, 0) = v_{20}(x) \geq 0, & x \in \Omega, t > 0. \end{cases} \quad (1.1)$$

It is model (1.1) that will be investigated in this paper.

The rest of this paper is organized as follows: In Section 2, we analyze the existence and local stability of equilibria and the related bifurcations of the model (1.1) in the absence of diffusion. In Section 3, we mainly consider the dynamic behaviours of the model with reaction-diffusion and deduce the condition for Turing instability. In Section 4, some numerical simulations are performed to verify the theoretical results we obtain. The results may reveal some potential patterns that are caused by fear induced by mature predators. We end this paper by Section 5, consisting of some conclusions and some discussions on the biological significance of our results as well as possible future investigations.

## 2. Prey-predator model (1.1) without diffusion

In this section, we investigate the temporal version of model (1.1) as follows:

$$\begin{cases} \frac{du}{dt} = \frac{ru}{1+k_1 v_2} \left(1 - \frac{u}{m}\right) - \frac{a u v_2}{b+u}, \\ \frac{dv_1}{dt} = \frac{c a u v_2}{b+u} - (\alpha + q_1) v_1, \\ \frac{dv_2}{dt} = \alpha v_1 - q_2 v_2^2. \end{cases} \quad (2.1)$$

### 2.1. Existence of equilibria

Obviously, model (2.1) has three types physical equilibria:

- (i) Trivial equilibrium  $E_0(0, 0, 0)$ , which always exists;
- (ii) The prey only equilibrium  $E_1(m, 0, 0)$ ;
- (iii) Coexistence equilibrium  $E^*(u^*, v_1^*, v_2^*)$ , if exists, satisfies

$$u^* = \frac{(\alpha + q_1) b q_2 v_2^*}{\alpha c - (\alpha + q_1) q_2 v_2^*}, \quad v_1^* = \frac{q_2 v_2^{*2}}{\alpha}. \quad (2.2)$$

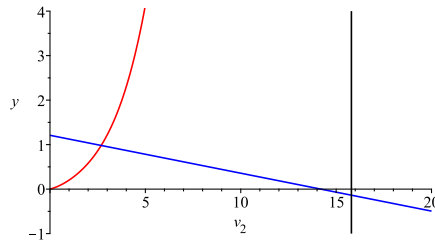


**Figure 1.** The graphs of functions  $f(v_2)$  and  $g(v_2)$ ; The blue curve stands for  $f(v_2)$ ; The red curve represents  $g(v_2)$ ; The black curve stands for  $v_2 = \frac{\alpha ac}{(\alpha + q_1)q_2}$ ; The parameters are set as  $r = 1.2, k_1 = 0.3, m = 9, a = 0.2, b = 1, c = 0.8, \alpha = 0.7, q_1 = 0.01, q_2 = 0.01$ .

Additionally,  $v_2^*$  can be solved from

$$\frac{(\alpha ac - (\alpha + q_1)q_2 v_2)v_2}{abc} = \frac{rm\alpha ac - (\alpha + q_1)(m + b)q_2 r v_2}{m(1 + k_1 v_2)(\alpha ac - (\alpha + q_1)q_2 v_2)}. \tag{2.3}$$

Clearly, (2.3) can be written as the following form:

$$\frac{(\alpha ac - (\alpha + q_1)q_2 v_2)^2(1 + k_1 v_2)mv_2}{abc} = rm\alpha ac - (\alpha + q_1)(m + b)q_2 r v_2. \tag{2.4}$$

Denote

$$f(v_2) = (\alpha ac - (\alpha + q_1)q_2 v_2)^2(1 + k_1 v_2)mv_2, \tag{2.5}$$

$$g(v_2) = abc(rm\alpha ac - (\alpha + q_1)(m + b)q_2 r v_2). \tag{2.6}$$

Notice first from (2.2) that  $u^* > 0$ , if and only if  $0 < v_2^* < \bar{v}_2 := \frac{\alpha ac}{(\alpha + q_1)q_2}$  and  $g(v_2)$  is a decreasing function with horizontal intercept  $\tilde{v}_2 := \frac{m\alpha ac}{(m + b)(\alpha + q_1)q_2}$ . It is easy to check that  $\tilde{v}_2 < \bar{v}_2$ . Then, the existence and number of coexistence equilibria can be determined by discussing the intersection of curves  $f(v_2)$  and  $g(v_2)$  over the interval  $(0, \bar{v}_2)$ . Since  $f(0) = 0 < (\alpha c)^2 abrm = g(0)$  and  $f(\tilde{v}_2) > 0 = g(\tilde{v}_2)$ , the curves  $f(v_2)$  and  $g(v_2)$  have at least one intersection in  $(0, \tilde{v}_2)$ . That is, model (2.1) has at least one coexistence equilibrium.

In Figure 1, we present a representative illustration of the coexistence equilibrium of model (2.1) for a set of fixed parameter values. The blue line stands for the curve of  $f(v_2)$ , the red line represents the curve of  $g(v_2)$  and the black vertical line is  $v_2 = \bar{v}_2$ . The intersection of the blue and red curves is  $v_2^*$  and model (2.1) has exactly one coexistence equilibrium  $E^*(u^*, v_1^*, v_2^*)$ .

To summarize, we have the following result.

**Theorem 2.1.** *Model (2.1) always has a trivial equilibrium  $E_0(0, 0, 0)$ , a prey only equilibrium  $E_1(m, 0, 0)$  and at least one coexistence equilibrium  $E^*(u^*, v_1^*, v_2^*)$ .*

### 2.2. Stability of equilibria

The Jacobian matrix at any equilibrium  $E(u, v_1, v_2)$  is given by

$$J(E) = \begin{pmatrix} a_{11} & 0 & a_{13} \\ a_{21} & a_{22} & a_{23} \\ 0 & a_{32} & a_{33} \end{pmatrix},$$

where

$$\begin{aligned} a_{11} &= \frac{r}{1+k_1v_2} - \frac{2ru}{m(1+k_1v_2)} - \frac{abv_2}{(b+u)^2}, \\ a_{13} &= -\frac{k_1ru}{(1+k_1v_2)^2} \left(1 - \frac{u}{m}\right) - \frac{au}{b+u}, \\ a_{21} &= \frac{abcv_2}{(b+u)^2}, \quad a_{22} = -(\alpha + q_1), \\ a_{23} &= \frac{acu}{b+u}, \quad a_{32} = \alpha, \quad a_{33} = -2q_2v_2. \end{aligned}$$

Now, we state the stability of the equilibria in following theorems.

**Theorem 2.2.** *The equilibrium  $E_0(0, 0, 0)$  is always unstable.*

**Proof.** Direct calculations lead to that the eigenvalues of Jacobian matrix  $J(E_0)$  are

$$\lambda_1 = r > 0, \quad \lambda_2 = -(\alpha + q_1) < 0, \quad \lambda_3 = 0, \quad (2.7)$$

which indicates that  $E_0(0, 0, 0)$  is always unstable.  $\square$

**Theorem 2.3.** *The equilibrium  $E_1(m, 0, 0)$  is always unstable.*

**Proof.** Direct calculations lead to that the eigenvalues of Jacobian matrix  $J(E_1)$  are

$$\begin{aligned} \lambda_1 &= -r < 0, \\ \lambda_2 &= \frac{-(\alpha + q_1) + \sqrt{(\alpha + q_1)^2 + \frac{4\alpha acm(\alpha + q_1)}{b+m}}}{2} > 0, \\ \lambda_3 &= \frac{-(\alpha + q_1) - \sqrt{(\alpha + q_1)^2 + \frac{4\alpha acm(\alpha + q_1)}{b+m}}}{2} < 0. \end{aligned}$$

Thus, the equilibrium  $E_1(m, 0, 0)$  is always unstable.  $\square$

At the positive equilibrium  $E^*(u^*, v_1^*, v_2^*)$ , the characteristic equation has the form

$$\lambda^3 + A\lambda^2 + B\lambda + C = 0, \quad (2.8)$$

where

$$\begin{aligned} A &= \frac{r(2u^* - m)}{m(1+k_1v_2^*)} + \frac{abv_2^*}{(b+u^*)^2} + (\alpha + q_1 + 2q_2v_2^*), \\ B &= (\alpha + q_1 + 2q_2v_2^*) \left\{ \frac{r(2u^* - m)}{m(1+k_1v_2^*)} + \frac{abv_2^*}{(b+u^*)^2} \right\} + 2q_2(\alpha + q_1)v_2^* - \frac{\alpha acu^*}{b+u^*}, \\ C &= \frac{\alpha acru^*(m - 2u^*)}{m(1+k_1v_2^*)(b+u^*)} + \frac{\alpha abck_1ru^*v_2^*}{(1+k_1v_2^*)^2(b+u^*)^2} \left(1 - \frac{u^*}{m}\right) \\ &\quad - 2(\alpha + q_1)q_2v_2^* \left\{ \frac{r}{1+k_1v_2^*} - \frac{2ru^*}{m(1+k_1v_2^*)} - \frac{abv_2^*}{(b+u^*)^2} \right\}. \end{aligned}$$

From Routh-Hurwitz criteria, we know that equation (2.8) will have negative roots or the roots with negative real parts, if

$$A > 0, \quad C > 0, \quad AB - C > 0. \quad (2.9)$$

Then, we have the following theorem.

**Theorem 2.4.** *The positive equilibrium  $E^*(u^*, v_1^*, v_2^*)$  is local stable, if the conditions in (2.9) are satisfied. Otherwise, it is unstable.*

In what follows, we discuss Hopf bifurcation for model (2.1) for the interior equilibrium point  $E^*(u^*, v_1^*, v_2^*)$  [11]. We will choose the fear level  $k_1$  as the bifurcation parameter.

**Theorem 2.5.** *The model (2.1) will undergo Hopf bifurcation around the interior equilibrium  $E^*(u^*, v_1^*, v_2^*)$ , when parameter  $k_1$  crosses the critical value  $k_1 = k_1^*$ , and the following conditions are satisfied:*

- (1)  $A(k_1^*), C(k_1^*) > 0$ ;
- (2)  $A(k_1^*)B(k_1^*) - C(k_1^*) = 0$ ;
- (3)  $C'(k_1^*) - A'(k_1^*)B(k_1^*) - A(k_1^*)B'(k_1^*) \neq 0$ .

**Proof.** As we know, Hopf bifurcation occurs when the characteristic equation has a pair of pure imaginary roots. Then, to determine the condition where Hopf bifurcation occurs for model (2.1), we assume that at the critical value  $k_1 = k_1^*$ , the roots of the characteristic equation (2.8) can be expressed as

$$\lambda_1(k_1) = i\phi_1(k_1^*), \quad \lambda_2(k_1) = -i\phi_1(k_1^*), \quad \lambda_3(k_1) = -\phi_2(k_1^*).$$

Substituting  $\lambda_1(k_1^*) = i\phi_1(k_1^*)$  into equation (2.8) and separating the real and imaginary components, we can get

$$\begin{cases} -A(k_1^*)\phi_1^2(k_1^*) + C(k_1^*) = 0, \\ -\phi_1^3(k_1^*) + B(k_1^*)\phi_1(k_1^*) = 0. \end{cases} \quad (2.10)$$

Solving (2.10), we obtain

$$\begin{cases} \phi_1^2(k_1^*) = \frac{C(k_1^*)}{A(k_1^*)}, \\ \phi_1^2(k_1^*) = B(k_1^*), \end{cases} \quad (2.11)$$

which indicates  $\frac{C(k_1^*)}{A(k_1^*)} = B(k_1^*)$ , i.e.,  $A(k_1^*)B(k_1^*) - C(k_1^*) = 0$ .

Now, we begin to examine the transversality condition. From (2.8), we have

$$\begin{aligned} \frac{d}{dk_1} [Re(\lambda(k_1))]_{k_1=k_1^*} &= \frac{B(k_1^*)C'(k_1^*) - A'(k_1^*)B^2(k_1^*) - A(k_1^*)B(k_1^*)B'(k_1^*)}{2(B^2(k_1^*) + A^2(k_1^*)B(k_1^*))}, \\ &= \frac{C'(k_1^*) - A'(k_1^*)B(k_1^*) - A(k_1^*)B'(k_1^*)}{2(B(k_1^*) + A^2(k_1^*))}. \end{aligned}$$

Then, when  $C'(k_1^*) - A'(k_1^*)B(k_1^*) - A(k_1^*)B'(k_1^*) \neq 0$ , the transversality condition is satisfied.  $\square$

### 3. Reaction-Diffusion prey-predator model

In the section, we perform the linear stability analysis for model (1.1) to discuss the influence of fear level on the spatiotemporal patterns of populations [12].

The linearized system of (1.1) at  $E^*(u^*, v_1^*, v_2^*)$  can be given by

$$\begin{cases} \frac{\partial u(x, t)}{\partial t} = d_{11}\Delta u(x, t) + a_{11}u(x, t) + a_{13}v_2(x, t), x \in \Omega, t > 0, \\ \frac{\partial v_1(x, t)}{\partial t} = d_{22}\Delta v_1(x, t) + a_{21}u(x, t) + a_{22}v_1(x, t) + a_{23}v_2(x, t), x \in \Omega, t > 0, \\ \frac{\partial v_2(x, t)}{\partial t} = d_{33}\Delta v_2(x, t) + a_{32}v_1(x, t) + a_{33}v_2(x, t), x \in \Omega, t > 0, \\ \frac{\partial u}{\partial \bar{v}} = 0, \frac{\partial v_1}{\partial \bar{v}} = 0, \frac{\partial v_2}{\partial \bar{v}} = 0, x \in \partial\Omega, t > 0, \\ u(x, 0) = u_0(x) \geq 0, v_1(x, 0) = v_{10}(x) \geq 0, v_2(x, 0) = v_{20}(x) \geq 0, x \in \Omega, t > 0, \end{cases} \quad (3.1)$$

where  $a_{ij}(i, j = 1, 2, 3)$  is evaluated at  $E^*(u^*, v_1^*, v_2^*)$ .

Let

$$u(x, t) = Ue^{\lambda t} \cos kx, \quad v_1(x, t) = V_1e^{\lambda t} \cos kx, \quad v_2(x, t) = V_2e^{\lambda t} \cos kx,$$

and substitute them into the system (3.1). Then, we can obtain the characteristic equation of (3.1)

$$\lambda^3 + D_k\lambda^2 + E_k\lambda + F_k = 0, \quad (3.2)$$

where

$$\begin{aligned} D_k &= (d_{11} + d_{22} + d_{33})k^2 - (a_{11} + a_{22} + a_{33}), \\ E_k &= (d_{11}k^2 - a_{11})(d_{22}k^2 - a_{22}) + (d_{11}k^2 - a_{11})(d_{33}k^2 - a_{33}) \\ &\quad + (d_{22}k^2 - a_{22})(d_{33}k^2 - a_{33}) - a_{23}a_{32}, \\ F_k &= (d_{11}k^2 - a_{11})(d_{22}k^2 - a_{22})(d_{33}k^2 - a_{33}) \\ &\quad - (d_{11}k^2 - a_{11})a_{23}a_{32} - a_{13}a_{21}a_{32}. \end{aligned}$$

In the rest of this section, we focus on Turing instability analysis [18, 22]. Turing theory implies that Turing instability occurs, if the constant equilibrium  $E^*$  is stable for model (2.1), and unstable for model (1.1). Therefore, in what follows, we assume that (2.9) holds.

When one of the eigenvalues passes through zero, the real parts of other two eigenvalues remain negative, Turing instability emerges [7]. Without any loss of generality, we use  $\tilde{\lambda}_1, \tilde{\lambda}_2$  and  $\tilde{\lambda}_3$  to represent the roots of the characteristic equation (3.2). Then, we obtain

$$\begin{aligned} \tilde{\lambda}_1 + \tilde{\lambda}_2 + \tilde{\lambda}_3 &= -D_k, \\ \tilde{\lambda}_1\tilde{\lambda}_2 + \tilde{\lambda}_2\tilde{\lambda}_3 + \tilde{\lambda}_1\tilde{\lambda}_3 &= E_k, \\ \tilde{\lambda}_1\tilde{\lambda}_2\tilde{\lambda}_3 &= -F_k. \end{aligned}$$

We use  $k_T$  to denote the critical wave number at Turing bifurcation threshold. Therefore, at the critical wave number  $k = k_T$ , we assume

$$\tilde{\lambda}_1|_{k^2=k_T^2} = 0, \quad Re(\tilde{\lambda}_2)|_{k^2=k_T^2} < 0 \quad \text{and} \quad Re(\tilde{\lambda}_3)|_{k^2=k_T^2} < 0. \quad (3.3)$$

Thus, we can get  $F_k = 0$  at the critical wave number  $k = k_T$ . Further, the conditions for Turing instability presented in (3.3) lead to  $D_k > 0, E_k > 0$  and  $D_kE_k - F_k =$

$D_k E_k > 0$ . Therefore, the coexistence steady state  $E^*$  is Turing unstable, when  $F_k < 0$  holds for at least one  $k > 0$ . Also, besides Turing bifurcation threshold, there exists a range  $k$ -values around  $k_T$  for which the inequality  $F_k < 0$  can hold true.

Let  $F_k = h(k^2)$ , then we have

$$h(k^2) = \tilde{A} \cdot (k^2)^3 + \tilde{B} \cdot (k^2)^2 + \tilde{C} \cdot k^2 + \tilde{D}, \tag{3.4}$$

where

$$\begin{aligned} \tilde{A} &= d_{11}d_{22}d_{33}, \\ \tilde{B} &= \left\{ \frac{2ru^*}{m(1+k_1v_2^*)} + \frac{abv_2^*}{(b+u^*)^2} - \frac{r}{1+k_1v_2^*} \right\} d_{11}d_{22} \\ &\quad + (\alpha + q_1)d_{11}d_{33} + 2q_2v_2^*d_{11}d_{22}, \\ \tilde{C} &= \left\{ \frac{2ru^*}{m(1+k_1v_2^*)} + \frac{abv_2^*}{(b+u^*)^2} - \frac{r}{1+k_1v_2^*} \right\} \{(\alpha + q_1)d_{33} + 2q_2v_2^*d_{22}\} \\ &\quad + \left\{ 2q_2v_2^*(\alpha + q_1) - \frac{\alpha acu^*}{b+u^*} \right\} d_{11}, \\ \tilde{D} &= \frac{\alpha acru^*(m-2u^*)}{m(1+k_1v_2^*)(b+u^*)} + \frac{\alpha abck_1ru^*v_2^*}{(1+k_1v_2^*)^2(b+u^*)^2} \left(1 - \frac{u^*}{m}\right) \\ &\quad - 2(\alpha + q_1)q_2v_2^* \left\{ \frac{r}{1+k_1v_2^*} - \frac{2ru^*}{m(1+k_1v_2^*)} - \frac{abv_2^*}{(b+u^*)^2} \right\}. \end{aligned}$$

As  $E^*$  is assumed to be stable, we have  $h(0) = \tilde{D} > 0$ . Furthermore,  $\tilde{A} = d_{11}d_{22}d_{33} > 0$  for positive diffusion coefficients, then  $h(k^2) \rightarrow \infty$  as  $k \rightarrow \infty$ . Hence, we need to find a little neighbourhood that has  $h(k^2) < 0$ , and Turing instability occurs at that time. If so, there should exist a local minimum value on  $0 < k^2 < \infty$ , and the minimum value should be less than zero. To achieve Turing instability, we seek  $k_{T_1}$  and  $k_{T_2}$  which satisfy

$$\frac{dh(k_{T_1}^2)}{dk_{T_1}^2} = \frac{dh(k_{T_2}^2)}{dk_{T_2}^2} = 0, \tag{3.5}$$

with  $k_{T_2} > 0$ ,

$$h(k_{T_2}^2) \leq 0. \tag{3.6}$$

Solving  $\frac{dh(k_{T_2}^2)}{dk_{T_2}^2} = 0$ , we obtain the formula for  $k_{T_1}$  and  $k_{T_2}$  in the terms of  $\tilde{A}$ ,  $\tilde{B}$ ,  $\tilde{C}$ , which are given by

$$k_{T_1}^2 = \frac{-\tilde{B} - \sqrt{\tilde{B}^2 - 3\tilde{A}\tilde{C}}}{3\tilde{A}}, \tag{3.7}$$

$$k_{T_2}^2 = \frac{-\tilde{B} + \sqrt{\tilde{B}^2 - 3\tilde{A}\tilde{C}}}{3\tilde{A}}. \tag{3.8}$$

To make sure that both  $k_{T_1}^2$  and  $k_{T_2}^2$  are real numbers, then we can get  $\tilde{B}^2 - 3\tilde{A}\tilde{C} > 0$ . In order to ensure  $k_{T_2}^2 > 0$ , we consider two cases: (i) if  $\tilde{B} > 0$ , then we require

$\tilde{C} < 0$ ; (ii) if  $\tilde{B} \leq 0$ , then we require  $\tilde{C} < \frac{\tilde{B}^2}{3\tilde{A}}$ . Assuming one of these cases holds and substituting  $k_{T_2}$  given by (3.8) into (3.4), and we get

$$h(k_{T_2}^2) = \frac{2\tilde{B}^2 - 9\tilde{A}\tilde{B}\tilde{C} - 2(\tilde{B}^2 - 3\tilde{A}\tilde{C})^{\frac{3}{2}} + 27\tilde{D}\tilde{A}^2}{27\tilde{A}^2}. \quad (3.9)$$

Therefore, we obtain the Turing bifurcation condition as

$$2\tilde{B}^2 - 9\tilde{A}\tilde{B}\tilde{C} - 2(\tilde{B}^2 - 3\tilde{A}\tilde{C})^{\frac{3}{2}} + 27\tilde{D}\tilde{A}^2 \leq 0. \quad (3.10)$$

Then, we have the following theorem.

**Theorem 3.1.** *If (3.10) can hold, model (1.1) undergoes Turing instability at  $E^*(u^*, v_1^*, v_2^*)$ .*

## 4. Numerical Simulations

In order to verify our theoretical results, we choose a two-dimensional space with  $200 \times 200$  grids. We employ the non-zero initial and Neumann boundary conditions to conduct all our numerical simulations. We set the space step and time step as  $\Delta h = 1$ ,  $\Delta t = 0.002$ . The initial density distributions are random spatial distributions of the species. In model (1.1),  $k_1$  denotes the fear level induced by the mature predators, and  $d_{33}$  stands for the diffusion coefficient of the mature predators. In this section, we will show the effect of the fear level induced by the mature predators and the diffusion coefficient of the mature predators on pattern formation. During the process of numerical simulations, the prey and predators always exhibit the same pattern structures. Hence, we only show the spatial distribution of the prey populations.

### 4.1. The effect of the varied $k_1$ on pattern formation

In this subsection, we fix  $a = 0.2$ ,  $b = 1$ ,  $c = 0.8$ ,  $q_1 = 0.01$ ,  $q_2 = 0.01$ ,  $\alpha = 0.7$ ,  $m = 9$ ,  $r = 1.2$ ,  $d_{11} = 0.2$ ,  $d_{22} = 0.1$ ,  $d_{33} = 20$ , and we choose different  $k_1$  to observe the dynamic behavior of model (1.1). We find that for different fear levels, there are five basic types of pattern structures: cold-spot pattern, mixed pattern with cold spots and stripes, stripes pattern, hot-spot pattern and mixed pattern with hot spots and stripes.

When  $k_1 = 0.027$ ,  $E^*(u^*, v_1^*, v_2^*) = (3.730, 2.211, 12.440)$ , and in the meantime the roots of equation (2.8) are  $-0.0217 \pm 0.0965i$ ,  $-0.8730$ , where  $i$  is the imaginary unit and  $i^2 = -1$ . That is,  $E^*(u^*, v_1^*, v_2^*)$  is linearly stable for the temporal version of model. However, equation (3.2) has a positive root, when the wave number  $k$  belongs to  $(0.125, 0.437)$ , which indicates that Turing patterns will occur. The spatiotemporal patterns of prey are shown in Figure 2, the prey populations show a cold-spot pattern, which suggests the prey species have lower population density and they will have less biological activities in the cold-spot domain.

As the fear level  $k_1$  increases, for example, when  $k_1 = 0.05$ ,  $E^*(u^*, v_1^*, v_2^*) = (0.899, 0.797, 7.467)$ , the roots of equation (2.8) are  $0.1094$ ,  $0.1418$  and  $-0.8256$ , and equation (3.2) has a positive root, when the wave number  $k$  belongs to  $(0.0563, 1.1914)$ . We present the evolution of prey in Figure 3, from which we can see that the mixed form of stripe patterns and cold spots emerges gradually, when  $t = 100$  and presents

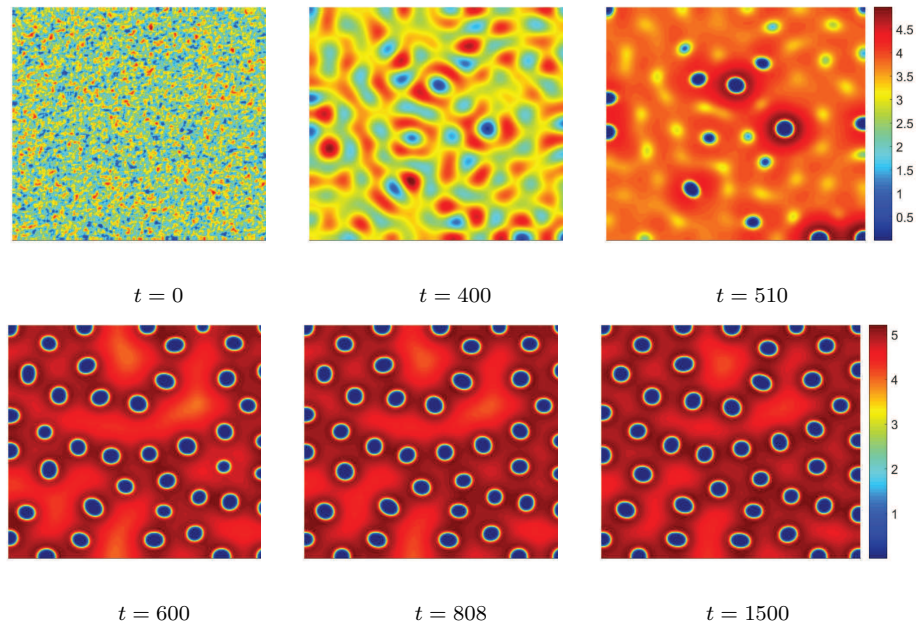


**Figure 2.** Evolution of the prey population at different instants with parameters  $k_1 = 0.027, a = 0.2, b = 1, c = 0.8, q_1 = 0.01, q_2 = 0.01, \alpha = 0.7, m = 9, r = 1.2, d_{11} = 0.2, d_{22} = 0.1, d_{33} = 20$

clearly, when  $t = 600$ . The mixed form is completely stable as  $t = 1500$ . When the fear level  $k_1 = 0.08$ ,  $E^*(u^*, v_1^*, v_2^*) = (0.633, 0.535, 6.117)$  and equation (3.2) has a positive root, when the wave number  $k$  belongs to  $(0.0703, 1.0779)$ . The evolution of prey is presented in Figure 4, from which we can see that the labyrinth pattern emerges gradually, when  $t = 160$  and presents clearly, when  $t = 800$ . The labyrinth pattern is completely stable as  $t = 1500$ . The dynamic behaviour of model (1.1) shows a change from spot-stripe growth to stripe pattern as  $k_1$  increases gradually like a labyrinth, i.e., cold-spot fades away and stripe pattern appears gradually.

As the fear level  $k_1$  increases into 0.135, the equilibrium  $E^*(u^*, v_1^*, v_2^*) = (0.46, 0.35, 4.97)$  and the roots of equation (2.8) are  $0.0817 \pm 0.1202i$  and  $-0.7949$ , and equation (3.2) has a positive root, when the wave number  $k$  belongs to  $(0.0819, 0.9392)$ . In this case, interesting situations occur. We present the evolution of prey in Figure 5, from which we can see that hot spots seem to present when  $t = 80$ , but almost disappear, when  $t = 120$ . When  $t = 260$ , hot spots present again, but almost disappear, when  $t = 284$ . Hot spots pattern present stable ultimately, when  $t = 1500$ . As  $k_1$  increases into 0.135, stripes have disappeared, and hot spots have emerged in the meantime. The circumstance indicates that the prey population gathers in the regions. From biological significance, the regions where the prey is plentiful are called colonies. They are ordinary in ecological models, as the colony formation allows the populations to be more effective in reproduction, feeding and defending risks.

When the fear level  $k_1$  reaches 0.14,  $E^*(u^*, v_1^*, v_2^*) = (0.45, 0.34, 4.90)$  and the roots of equation (2.8) are  $0.0801 \pm 0.1211i$  and  $-0.7939$ , and equation (3.2) has a positive root, when the wave number  $k$  belongs to  $(0.0826, 0.9295)$ , Turing pattern is different from the above discussion again. In Figure 6, when  $t = 360$ , hot stripes

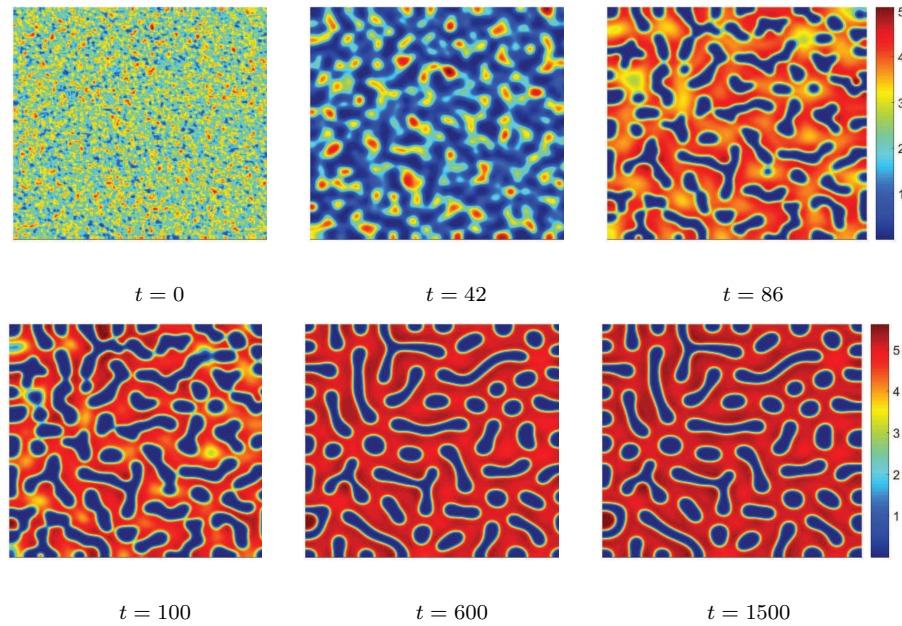


**Figure 3.** Evolution of the prey population at different instants with parameters  $k_1 = 0.05$ ,  $a = 0.2$ ,  $b = 1$ ,  $c = 0.8$ ,  $q_1 = 0.01$ ,  $q_2 = 0.01$ ,  $\alpha = 0.7$ ,  $m = 9$ ,  $r = 1.2$ ,  $d_{11} = 0.2$ ,  $d_{22} = 0.1$ ,  $d_{33} = 20$ .

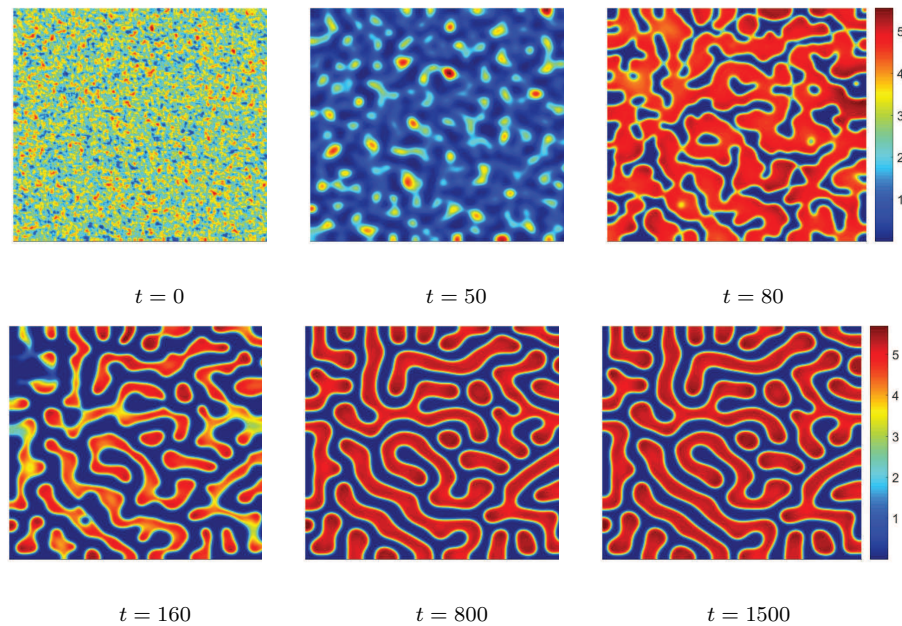


**Figure 4.** Evolution of the prey population at different instants with parameters  $k_1 = 0.08$ ,  $a = 0.2$ ,  $b = 1$ ,  $c = 0.8$ ,  $q_1 = 0.01$ ,  $q_2 = 0.01$ ,  $\alpha = 0.7$ ,  $m = 9$ ,  $r = 1.2$ ,  $d_{11} = 0.2$ ,  $d_{22} = 0.1$ ,  $d_{33} = 20$ .

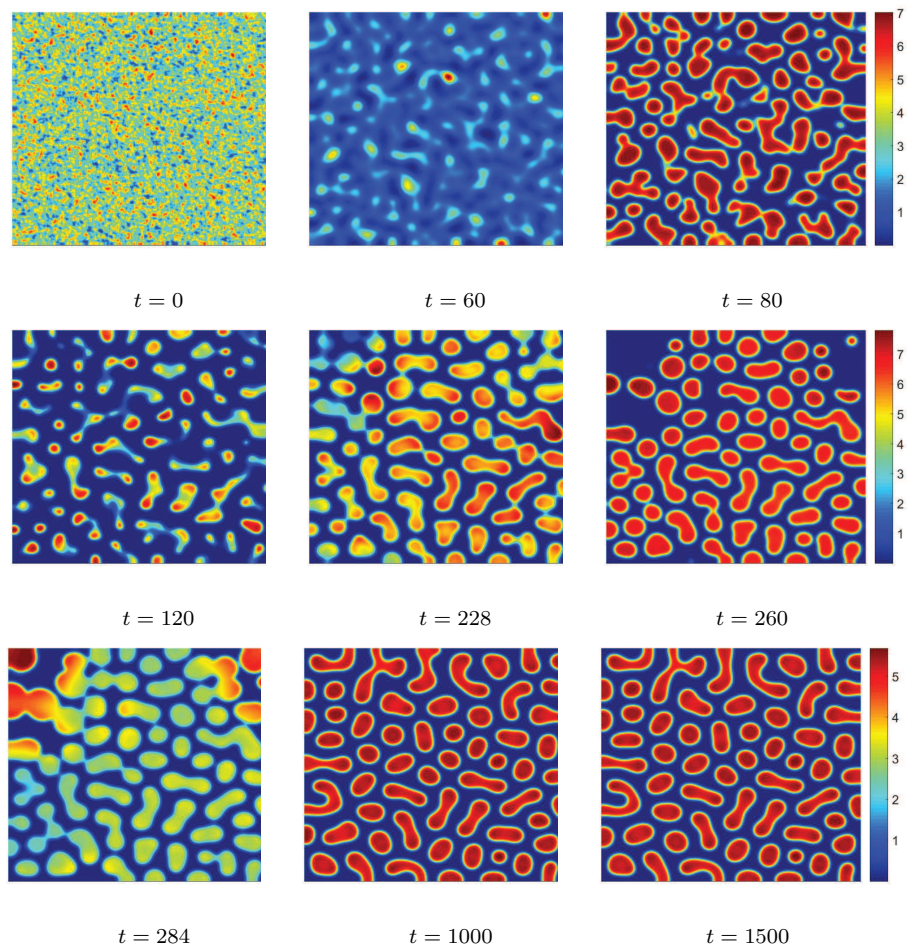


**Figure 5.** Evolution of the prey population at different instants with parameters  $k_1 = 0.135, a = 0.2, b = 1, c = 0.8, q_1 = 0.01, q_2 = 0.01, \alpha = 0.7, m = 9, r = 1.2, d_{11} = 0.2, d_{22} = 0.1, d_{33} = 20$

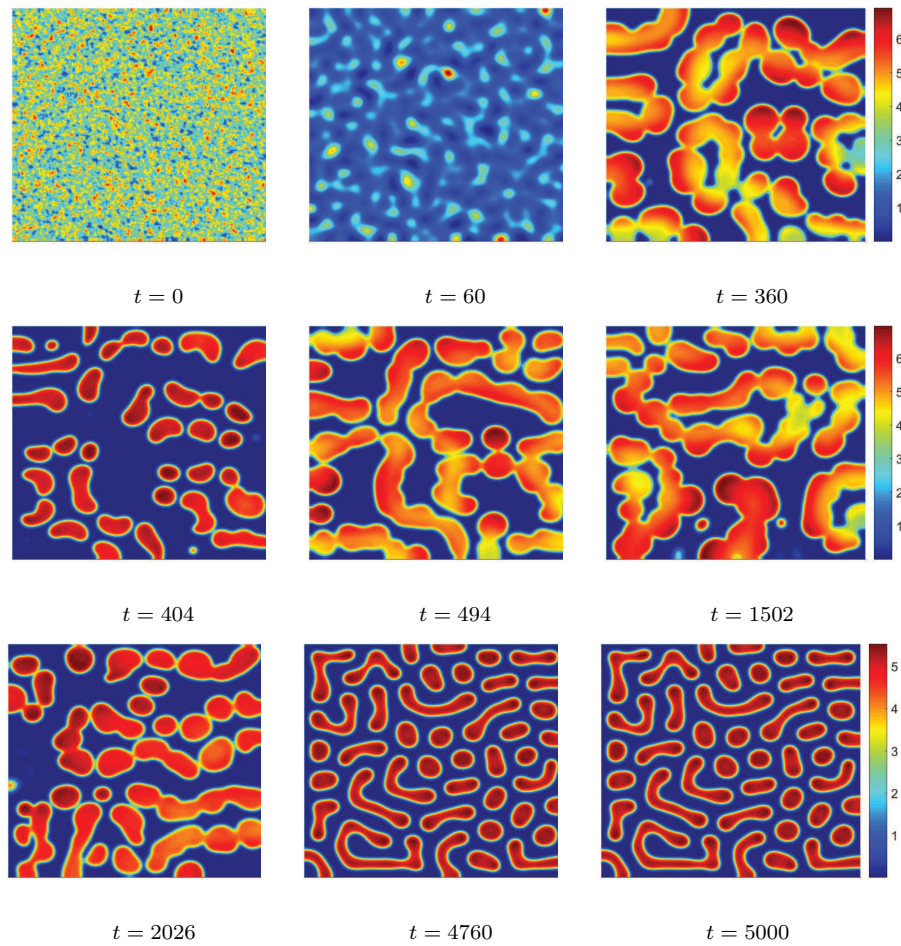


**Figure 6.** Evolution of the prey population at different instants with parameters  $k_1 = 0.14$ ,  $a = 0.2$ ,  $b = 1$ ,  $c = 0.8$ ,  $q_1 = 0.01$ ,  $q_2 = 0.01$ ,  $\alpha = 0.7$ ,  $m = 9$ ,  $r = 1.2$ ,  $d_{11} = 0.2$ ,  $d_{22} = 0.1$ ,  $d_{33} = 20$ .

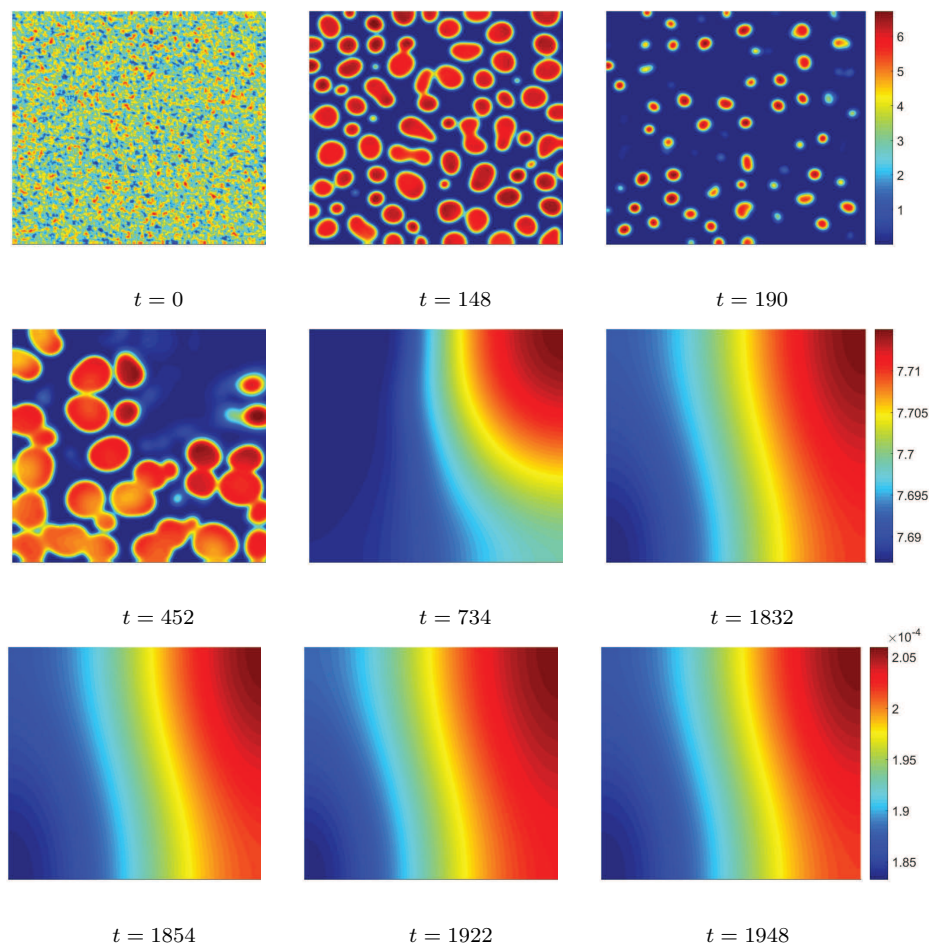


**Figure 7.** Evolution of the prey population at different instants with parameters  $k_1 = 0.3, a = 0.2, b = 1, c = 0.8, q_1 = 0.01, q_2 = 0.01, \alpha = 0.7, m = 9, r = 1.2, d_{11} = 0.2, d_{22} = 0.1, d_{33} = 20$ .

seem to present. However, when  $t = 404$ , Turing pattern seems to become hot spots. Gradually increase over time, hot stripes present again, when  $t = 1502$ . Turing pattern present stable ultimately, when  $t = 5000$ . From Figure 6, we can see that hot spot also exists, but in the meantime some stripes have emerged, i.e., mixed pattern with hot spots and stripes.

On the above analysis, we have considered the situation where the fear level  $k_1$  is smaller, and we can see the model shows abundant kinetics phenomenon. However, when  $k_1$  becomes a little bigger, what behaviour will happen? We have also done some numerical simulations, which indicates that when  $k_1 > 0.3$ , Turing pattern will disappear. The results presented in Figure 7 show that the densities of preys and predators change periodically over time.

### 4.2. The effect of the varied $d_{33}$ on pattern formation

In biology, self-diffusion is one of the vital factors causing Turing instability for model (1.1). In this subsection, we consider self-diffusion of mature predators and

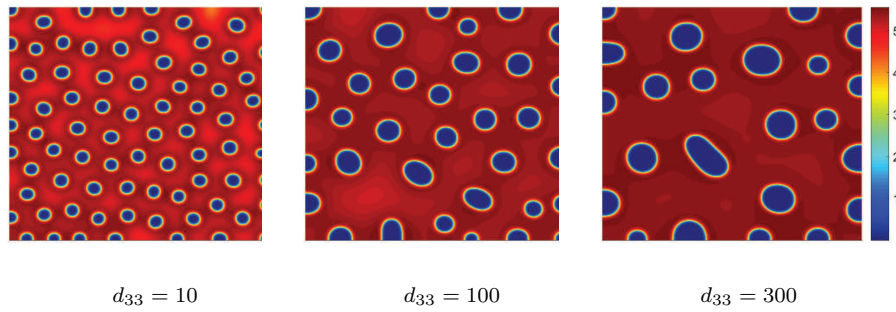


**Figure 8.** The three categories of Turing pattern of the prey population at  $t = 1000$  with different self-diffusion of the mature predators  $d_{33}$ . Fixing  $a = 0.2, b = 1, c = 0.8, q_1 = 0.01, q_2 = 0.01, \alpha = 0.7, m = 9, r = 1.2, k_1 = 0.028, d_{11} = 0.2, d_{22} = 0.1, t = 1000$ , and we choose different  $d_{33}$  to observe the patterns.

conduct some numerical simulations. We fix  $a = 0.2, b = 1, c = 0.8, q_1 = 0.01, q_2 = 0.01, \alpha = 0.7, m = 9, r = 1.2, d_{11} = 0.2, d_{22} = 0.1$ , and select different values  $d_{33} = 10, 100, 300$  to observe the results. From Figure 8, we can see that as the increase of the self-diffusion of mature predators, the cold spots become fewer but bigger. As the increase of diffusion coefficients of the mature predators, the prey populations are more tightly packed together. Therefore, we can observe that the population density of prey becomes even enhanced, but the size of spots becomes bigger. This phenomenon suggests that when the diffusion coefficient of the mature predators becomes faster, which can impact on the densities of the prey species, the prey will tend to bond more closely to defend the predation from mature predators.

## 5. Conclusion and discussion

In this paper, we consider a fearful predator-prey model in which the predators are divided into juvenile and mature predators. The fear perceived by prey is assumed to only come from the mature predators. In the absence of diffusion, we discuss the existence and stability of equilibria of the temporal model. Also, we deduce the critical conditions of Hopf bifurcation for model (1.1) without diffusion and Turing bifurcation for model (1.1).

We choose the fear level  $k_1$  induced by the mature predators as bifurcation parameter to reveal the influences of model (1.1) on the pattern dynamics. More specifically, when the fear level  $k_1 = 0.027$ , model (1.1) presents cold spot pattern as shown in Figure 2, when  $k_1 = 0.05$ , prey presents cold spot-stripe pattern as shown in Figure 3. When  $k_1 = 0.08$ , prey shows labyrinth pattern as shown in Figure 4; When  $k_1 = 0.135$ , prey presents hot spot pattern as shown in Figure 5, which suggests that the prey population is concentrated, and in this way, the prey can spawn and guard together, which pattern may be helpful for the living of the prey population. When  $k_1 = 0.14$ , model (1.1) presents hot spot-stripe pattern as shown in Figure 6. When  $k_1 = 0.3$ , model (1.1) cannot present pattern, but the densities of prey and predators change periodically over time, which indicates when  $k_1$  is large, Hopf bifurcation is dominant in the dynamic behaviors of model (1.1). Additionally, in the real world, self-diffusion of the mature predators is one of the vital factors affects pattern formation. Therefore, we also choose  $d_{33}$  to conduct

numerical simulations. From Figure 8, we can see that the spot patterns grow larger in size, but become far fewer in number as  $d_{33}$  increases. This suggests the prey tends to scatter less, as the mature predators disperse more efficiently.

The results obtained in this paper can help one better understand the dynamic behaviors of prey-predator model and enrich the research of pattern formation. However, further analysis are also necessary to study the dynamic behaviour of more complex spatial models such as stage-structured prey-predator models with delay, noise, cross-diffusion or other terms [16, 19].

## Acknowledgments

The authors express their sincere gratitude to the editors and reviewers for their helpful comments and suggestions.

## References

- [1] W. G. Aiello and H. I. Freedman, *A time-delay model of single-species growth with stage structure*, *Mathematical Biosciences*, 1990, 101(2), 139–153.
- [2] S. J. Brentnall, K. J. Richards, J. Brindley and E. Murphy, *Eugene Murphy, Plankton patchiness and its effect on larger-scale productivity*, *Journal of Plankton Research*, 2003, 25(2), 124–140.
- [3] S. Creel and D. Christianson, *Relationships between direct predation and risk effects*, *Trends in Ecology & Evolution*, 2008, 23(4), 194–201.
- [4] W. Cresswell, *Predation in bird populations*, *Journal of Ornithology*, 2011, 152, 251–263.
- [5] S. Gakkhar and K. Gupta, *Dynamics of a Stage-Structured Predator-Prey Model*, *International Journal of Applied Physics and Mathematics*, 2017, 7(1), 24–32.
- [6] C. Holling, *Some Characteristics of Simple Types of Predation and Parasitism*, *The Canadian Entomologist*, 1959, 91(7), 385–398.
- [7] Q. Li, Z. Liu and S. Yuan, *Cross-diffusion induced Turing instability for a competition model with saturation effect*, *Applied Mathematics and Computation*, 2019, 347, 64–77.
- [8] S. L. Lima, *Nonlethal Effects in the Ecology of Predator-Prey Interactions*, *BioScience*, 1998, 48(1), 25–34.
- [9] S. L. Lima, *Predators and the breeding bird: behavioral and reproductive flexibility under the risk of predation*, *Biological Reviews*, 2009, 84, 485–513.
- [10] Y. Lu, A. Kasia and S. Liu, *A stage-structured predator-prey model with predation over juvenile prey*, *Applied Mathematics and Computation*, 2017, 297, 115–130.
- [11] J. D. Murray, *Mathematical Biology I: An Introduction*, Springer, Berlin, 2002.
- [12] J. D. Murray, *Mathematical Biology II: Spatial Models and Biomedical Application*, Springer, Berlin, 2003.
- [13] S. D. Peacor, B. L. Peckarsky and G. C. Trussell and J. R. Vonesh, *Costs of predator-induced phenotypic plasticity: a graphical model for predicting the*

- contribution of nonconsumptive and consumptive effects of predators on prey*, *Oecologia*, 2013, 171, 1–10.
- [14] N. Pettorelli, T. Coulson and S. M. Durant and J. M. Gaillard, *Predation, individual variability and vertebrate population dynamics*, *Oecologia*, 2011, 167, 305–314.
- [15] R. J. Power and R. X. S. Compion, *Lion predation on elephants in the Savuti, Chobe National Park, Botswana*, *African Zoology*, 2009, 44(1), 36–44.
- [16] G. Sun, Z. Jin, Q. Liu and B. Li, *Rich dynamics in a predator–prey model with both noise and periodic force*, *Biosystems*, 2010(1), 100, 14–22.
- [17] T. O. Svernungsen, O. H. Holen and O. Leimar, *Inducible Defenses: Continuous Reaction Norms or Threshold Traits?*, *The American Naturalist*, 2011, 178(3), 397–410.
- [18] A. M. Turing, *The Chemical Basis of Morphogenesis*, *Philosophical Transactions of the Royal Society of London. Series B, Biological Sciences*, 1952, 237(641), 37–72.
- [19] C. Wang, S. Yuan and H. Wang, *Spatiotemporal patterns of a diffusive prey–predator model with spatial memory and pregnancy period in an intimidatory environment*, *Journal of Mathematical Biology*, 2022, 84(3), 12, 36 pages.
- [20] X. Wang and X. Zou, *Modeling the Fear Effect in Predator–Prey Interactions with Adaptive Avoidance of Predators*, *Bulletin of Mathematical Biology*, 2017, 79, 1325–1359.
- [21] F. Wei, C. Wang and S. Yuan, *Spatial Dynamics of a Diffusive Predator-prey Model with Leslie-Gower Functional Response and Strong Allee Effect*, *Journal of Nonlinear Modeling and Analysis*, 2020, 2(2), 267–285.
- [22] S. Xu, M. Qu and C. Zhang, *Investigating the Turing Conditions for Diffusion-driven Instability in Predator-prey System with Hunting Cooperation Functional Response*, *Journal of Nonlinear Modeling and Analysis*, 2021, 3(4), 663–676.
- [23] W. Yao and X. Li, *Bifurcation Difference Induced by Different Discrete Methods in a Discrete Predator-prey Model*, *Journal of Nonlinear Modeling and Analysis*, 2022, 4(1), 64–79.
- [24] L. Y. Zanette, A. F. White, M. C. Allen and M. Clinchy, *Perceived Predation Risk Reduces the Number of Offspring Songbirds Produce per Year*, *Science*, 2011, 334(6061), 1398–1401.
- [25] S. Zhang, S. Yuan and T. Zhang, *A predator-prey model with different response functions to juvenile and adult prey in deterministic and stochastic environments*, *Applied Mathematics and Computation*, 2021, 413, Article ID 126598, 26 pages.
- [26] S. Zhang, T. Zhang and S. Yuan, *Dynamics of a stochastic predator–prey model with habitat complexity and prey aggregation*, *Ecological Complexity*, 2021, 45, Article ID 100889, 13 pages.